Regional Climate Simulations over North America: Interaction of Local Processes with Improved Large-Scale Flow

GONZALO MIGUEZ-MACHO, GEORGIY L. STENCHIKOV, AND ALAN ROBOCK

Department of Environmental Sciences, Rutgers University, New Brunswick, New Jersey

(Manuscript received 14 October 2003, in final form 6 August 2004)

ABSTRACT

The reasons for biases in regional climate simulations were investigated in an attempt to discern whether they arise from deficiencies in the model parameterizations or are due to dynamical problems. Using the Regional Atmospheric Modeling System (RAMS) forced by the National Centers for Environmental Prediction–National Center for Atmospheric Research reanalysis, the detailed climate over North America at 50-km resolution for June 2000 was simulated. First, the RAMS equations were modified to make them applicable to a large region, and its turbulence parameterization was corrected. The initial simulations showed large biases in the location of precipitation patterns and surface air temperatures. By implementing higher-resolution soil data, soil moisture and soil temperature initialization, and corrections to the Kain–Fritch convective scheme, the temperature biases and precipitation amount errors could be removed, but the precipitation location errors remained. The precipitation location biases could only be improved by implementing spectral nudging of the large-scale (wavelength of 2500 km) dynamics in RAMS. This corrected for circulation errors produced by interactions and reflection of the internal domain dynamics with the lateral boundaries where the model was forced by the reanalysis.

1. Introduction

Climate change simulations conducted using conventional global general circulation models (GCMs) with a relatively coarse spatial resolution do not resolve important regional features. Their simulations of climate change on a regional scale are very uncertain, and these regional uncertainties are an important obstacle to the assessment of the impacts of climate change on society. Therefore, climate downscaling has important practical applications. There are two major approaches to this problem: statistical and dynamical. Here we focus on dynamical downscaling.

Relatively fine-resolution climate integrations can be produced with global models in a reasonable time, but present computer resources and the number of experiments needed for a study still make GCMs impractical for regional climate applications. One approach to produce high-resolution climate simulations is to nest a mesoscale model within a general circulation model over an area of interest (Dickinson et al. 1989; Giorgi 1990). The regional model is run at finer resolution than the global model to generate small scales absent in the global model fields. They are necessary to simulate mesoscale processes and their effects on local climate. These small scales of the atmospheric variables are produced by better representing interaction with topography and land cover heterogeneities, by resolving growing instabilities in the flow, and by better simulating convective processes (even though resolution may not be sufficient to resolve convective cells). As a drawback, lateral boundary conditions required to drive a limited-area model add a factor of uncertainty absent in global models, because they pose a constraint to the dynamics that interferes with the solution (Warner et al. 1997; Staniforth 1997). One way to avoid the boundary condition problem is to use a global model with enhanced resolution over the area of interest, either by grid stretching (Fox-Rabinovitz et al. 2000) or by rotating the pole (Wang et al. 1999). However, the nested approach is more economical, and in this study, we will use it for climate downscaling.

The nested model technique is used routinely for short-to-medium-range weather prediction, but its extension for simulations lasting extended periods of time to produce climate statistics is relatively new and is the subject of active research and controversy. Giorgi and Mearns (1999), for example, present an overview of several issues regarding regional climate modeling. It often happens that models that show relatively good skill at forecasts up to a few days exhibit large biases

Corresponding author address: Prof. Alan Robock, Department of Environmental Sciences, Rutgers University, 14 College Farm Road, New Brunswick, NJ 08901.
E-mail: robock@envsci.rutgers.edu

when run in climate mode, and these biases are accentuated in summer integrations, when boundary forcings are weaker. These mixed results have brought skepticism about the limitations of the nested model approach for climate simulations, not just because of more development needed in the models, but also because of problems arising from the technique itself. One of these problems is the dependence of results, including sensitivities, on the size of the domain (Seth and Giorgi 1998).

Several studies that evaluated regional simulations for the present climate (Christensen et al. 1997; Hong and Leetmaa 1999; Takle et al. 1999; Liang et al. 2001; Frei et al. 2003; Anderson et al. 2003; among others) speculated about the causes of the model bias. They do this despite the difficulty of attribution of errors to one parameterization or component of the model, as a result of the complex feedbacks occurring in the climate system and the cancellation of errors that can often happen when tuning a model.

Noguer et al. (1998) performed regional climate simulations using GCM data or data produced by the same GCM relaxed continuously to operational analysis to discern whether errors in the regional climate model simulations are due to the model or the boundary data. They found that in the winter, when boundary forcing is strongest, about 60% of the error variance for temperature and 40% for precipitation were due to errors from the boundary conditions. However, in the summer, the regional model produced similar biases when driven by either the GCM or the GCM relaxed to analysis data, and the errors were also different from the errors already present in the GCM simulation. They concluded that in the summer, when boundary forcings are weaker, the regional climate is largely responsible for the climate bias.

The effect of the constraint in the boundaries grows with time as the nested model evolves differently than the model that supplies the boundary data. This divergent behavior could be attributed to the chaotic nature of the flow or to deficiencies in one or both models. Denis et al. (2002) showed that the nested model approach in climate mode for a winter simulation produces good results when the model used to provide the boundary data and initial data is the same as the nested model and is run with the same resolution over a larger domain. In this study, the data produced by the same model at the same resolution were filtered to eliminate small scales and emulate the use of relatively coarse atmospheric reanalysis or GCM data often used to initialize and drive the nested models. Denis et al. (2002) concluded that a major component of the differences between the climate statistics from a nested model simulation and those from the fields used to drive the model from the boundaries can be attributed to formulation differences between the nested model and the model that produced the boundary conditions, and not to the chaotic nature of the flow or the nesting technique itself. When using verifying analyses as initial and boundary conditions, the differences are then due mostly to nested model deficiencies.

If a climate bias can be assigned to model deficiencies for the most part, the nested model approach for climate simulations can be used as an important tool to improve models, since the results do not depend as much on initial conditions, such as with short-term weather prediction, and misrepresented processes in the model become more apparent. That a region is isolated as the model domain also limits the number of feedbacks with distant regions and climate interactions that occur in a GCM simulation. However, the possibility that some aspects of the nesting technique, like the imposed boundary conditions and their interaction with the model dynamics, may play an important role in the model bias cannot be discarded and needs to be explored in greater detail.

Our goal is to set up a regional model [Regional Atmospheric Modeling System (RAMS)] for climate applications over North America. RAMS is a compressible nonhydrostatic model and was originally designed for small domains and short-term applications. As a first stage, we performed summer simulations with boundary conditions from National Centers for Environmental Prediction–National Center for Atmospheric Research (NCEP–NCAR) reanalysis, and preliminary results showed that the climate from the model differed considerably from observations. The main objective of this study is not only to describe the biases, but also to try to identify what factors contribute to create them, and to describe some improvements implemented in the model in order to have them corrected. Our experiments are also intended to reveal what components of the bias cannot be expected to change despite all modifications in the model parameterizations and which can therefore be attributed to the nesting technique.

In the process of obtaining a satisfactory solution, we evaluated the sensitivity of the simulation to several components of the model, focusing on improvements of the soil–vegetation model and convective parameterization, as well as the effect of the regional circulation on the precipitation patterns. In some experiments, a spectral nudging technique, in which long waves of the atmospheric fields are relaxed to reanalysis, was used to keep the large-scale circulation close to reanalysis and in this manner helped to identify the source of the bias appearing in the results. The relaxation of the long waves in the domain to those of the driving fields with a spectral nudging technique was first proposed for a limited-area model by Waldron et al. (1996), and it has been applied to regional climate simulations by von Storch et al. (2000). More recently, Miguez-Macho et al. (2004) showed that spectral nudging of the long waves eliminates the unphysical dependence of regional modeling results (especially precipitation) on the position and size of the domain.

We found that dynamic interactions of long waves initiated by the boundary conditions and long waves originating in the domain could produce a spurious wave structure that significantly affects physical processes in the domain. This effect has been mostly overlooked in many previous studies, and it is an intrinsic feature of the nesting technique itself. This suggests that the nesting setup chosen for long-term climate simulations should be critically tested in terms of propagation of long waves in the domain. We found that gentle spectral nudging improves the result significantly, correcting the phases of the first few long waves in the domain.

The paper is organized as follows. Section 2 briefly describes the model and changes implemented in its formulation mainly to adapt the model for large domains, together with the setup for the experiments. Section 3 evaluates a preliminary simulation of the model. In section 4, we assess the relative importance of land–air interaction processes, and in section 5, we assess the relative influence of the convective parameterization. Finally, in section 6, we evaluate the impact of aspects of the dynamics; we discuss the spectral nudging technique implemented in the model to keep the large scale close to reanalysis and possible reasons for the dynamical biases, which we link to the presence of the lateral boundaries. In section 7, we present a summary and conclusions.

2. Model and experimental setup

The model used in the experiments is RAMS version 4.3, a compressible nonhydrostatic model that was developed originally at Colorado State University (Pielke et al. 1992; Cotton et al. 2003). RAMS uses a terrain-following sigma-z coordinate (Gal-Chen and Somerville 1975) and a hybrid implicit-in-the-vertical time-split differencing scheme (Tripoli and Cotton 1982). It has several options for turbulence closure and radiation. The soil–vegetation model in RAMS is the Land Ecosystem–Atmosphere Feedback model (LEAF-2; Walko et al. 2000), which prognoses temperature and water content of the soil, snow cover, vegetation, and canopy air, and turbulent and radiative exchanges between these components. LEAF-2 uses a mosaic approach where the grid cells are subdivided into smaller portions or "patches" corresponding to different surface characteristics occurring in the area covered by the grid cell.

The domain and topography utilized in the experiments are shown in Fig. 1. The eastern and western boundaries are well into the ocean, minimizing vertical interpolation problems of the boundary conditions to the sigma levels of RAMS. The southern boundary approximately follows latitude 15°N, and the Gulf of Mexico is entirely included in the model domain. The grid spacing used in the experiments is 50 km (150 × 108 points) in the horizontal and variable in the vertical, with 30 levels up to a height surpassing 20 km. The resolution is higher in the boundary layer, with the first level at about 50 m above the ground and 10 levels in the first 1500 m. The buffer zone in the boundaries comprises 15 points and stays over the ocean on the east and west of the domain. The relaxing coefficient follows a parabolic function and is constant with height, as is standard in RAMS. Initial and boundary condi-

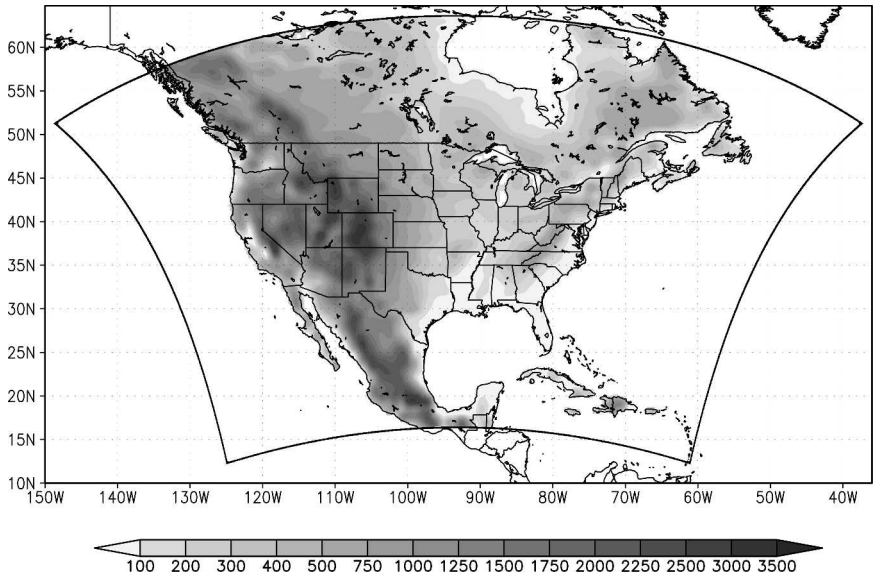

FIG. 1. Domain and topography utilized in the experiments. Curved lines indicate the outer boundary of the "box" for RAMS where it is driven by the reanalysis. Shading indicates elevation (m).

tions are from NCEP–NCAR reanalysis I (Kalnay et al. 1996) and the nesting interval is 6 h.

RAMS was originally designed, and has been mainly applied, for research in mesoscale and cloud-scale processes. To adapt the model to large domains, we found it necessary to remove the assumption that deviations of temperature from the reference state are negligible compared to the reference state temperature values in the momentum equations. The reference states in RAMS are constant in time and horizontally homogeneous, and vary with elevation above sea level. The removal of this simplification implies the inclusion of new pressure gradient force terms in the horizontal as well as in the vertical, whose absence had caused artificial stretching effects of atmospheric vortexes and errors in pressure calculations, especially in the center of cold core storms (results not shown).

Background density is also allowed to vary horizontally and in time, as deviations from the reference state are considered for our experiments. The effect of this change is smaller than the effect of perturbation temperature terms in the momentum equations.

In addition, turbulent kinetic energy has been restricted above the boundary layer (with a maximum limit of 1 $m^2 s^{-2}$ for heights above about 2000 m above the surface and a maximum of 10 $m^2 s^{-2}$ below that level). This is necessary to prevent unrealistic high values produced by the Mellor–Yamada scheme, which had resulted in large unphysical vertical mixing coefficients in the midtroposphere.

3. Preliminary experiment

We thoroughly tested the model after the aforementioned changes, and here we examine the model climate with the options that have given good results for other short-term simulations and that are recommended in the manual of the model. The convective parameterization is the Kain–Fritsch (KF) scheme (Kain and Fritsch 1990); there is no explicit microphysics, and cloud water concentration is diagnosed; a "dump bucket" scheme is used for stratiform precipitation as in a climate version of RAMS (ClimRAMS; Liston and Pielke 2000); the subgrid turbulence model is from Mellor and Yamada (1974); and for radiation we use the two-stream delta-Eddington radiative transfer scheme of Harrington (1997). The soil model is set up with 11 layers to a depth of 2.5 m; soil textures are homogeneous horizontally as well as vertically and correspond to silty clay loam; initial soil moisture is 50% of saturation throughout the domain, which for this type of soil corresponds to a volumetric value of 0.232 $m^3 m^{-3}$; initial soil temperatures are derived from the initial temperatures at the lowest atmospheric level by subtracting values of the order of 5°C for the deeper layers and 1°–2°C for intermediate layers and by adding 1°–2°C for the layers closest to the surface. This procedure is the standard initialization method used in RAMS when the soil temperatures are not explicitly specified by the user at every grid point. We used weekly averages of sea surface temperatures at 1° latitude–longitude resolution (Reynolds et al. 2002).

Figure 2 shows results of this preliminary simulation for June 2000 (initialized 1 June at 0000 UTC). This month was characterized by frequent wave activity in the circulation over North America, particularly in the second half, which resulted in intense convection and large precipitation amounts over the Great Plains. Rainfall was scarcer over the southeastern United States, enhancing existing precipitation deficits and drought conditions over the region. The observed precipitation from gridded analysis at 0.25° × 0.25° resolution of the Unified Rain-gauge Dataset produced by the Climate Prediction Center of NCEP (Higgins et al. 2000) is shown in Fig. 2a. Figure 2b shows the RAMS monthly averaged precipitation. Precipitation from the model clearly differs from the observations in amount and in pattern. In the observations, precipitation has a maximum in the west Central Plains, reaching 11 mm day^{-1}, and presents a wide band pattern that goes from Texas to the Great Lakes in a south to north-northeast direction. In the rest of the United States, precipitation is much reduced, especially in the west and the interior southeast. In the model, maximum amounts are found in the eastern United States, around the Appalachians, and the bandlike structure of precipitation, which is also present, is tilted in a more west-to-east direction, with values in the Central Plains considerably reduced. Coastal precipitation, and rainfall around the Gulf of Mexico, including Florida, is practically absent in the model simulation.

Figure 3 shows average 2-m air temperature differences between the model and NCEP–NCAR reanalysis. Temperatures also exhibit large biases, being much warmer than the reanalysis (up to 4°C) throughout most of the continental areas. In the mountainous areas of the West, the differences are due largely to different topographic resolution.

The regional model approach is used to recreate small scales not present in the boundary and initial fields, and the model is supposed to do so mainly by better representing land–air interactions due to topography and heterogeneity of the land cover. From this initial experiment, we see that the model actually creates a more small-scale structure than is present in the reanalysis fields used in the boundaries (Fig. 3) or in the precipitation produced by the model that created those boundary fields. However, RAMS in this configuration develops large biases. The spatial correlation between precipitation results from this experiment and the observations over the U.S. area east of the Rockies (between 20° and 48°N and 100° and 75°W) is only 0.19, and the root-mean-square error over the same region is 80 mm. In the next section, we investigate the effect of modifications in the lower boundary representation, as we proceed to improve the model climate. The purpose

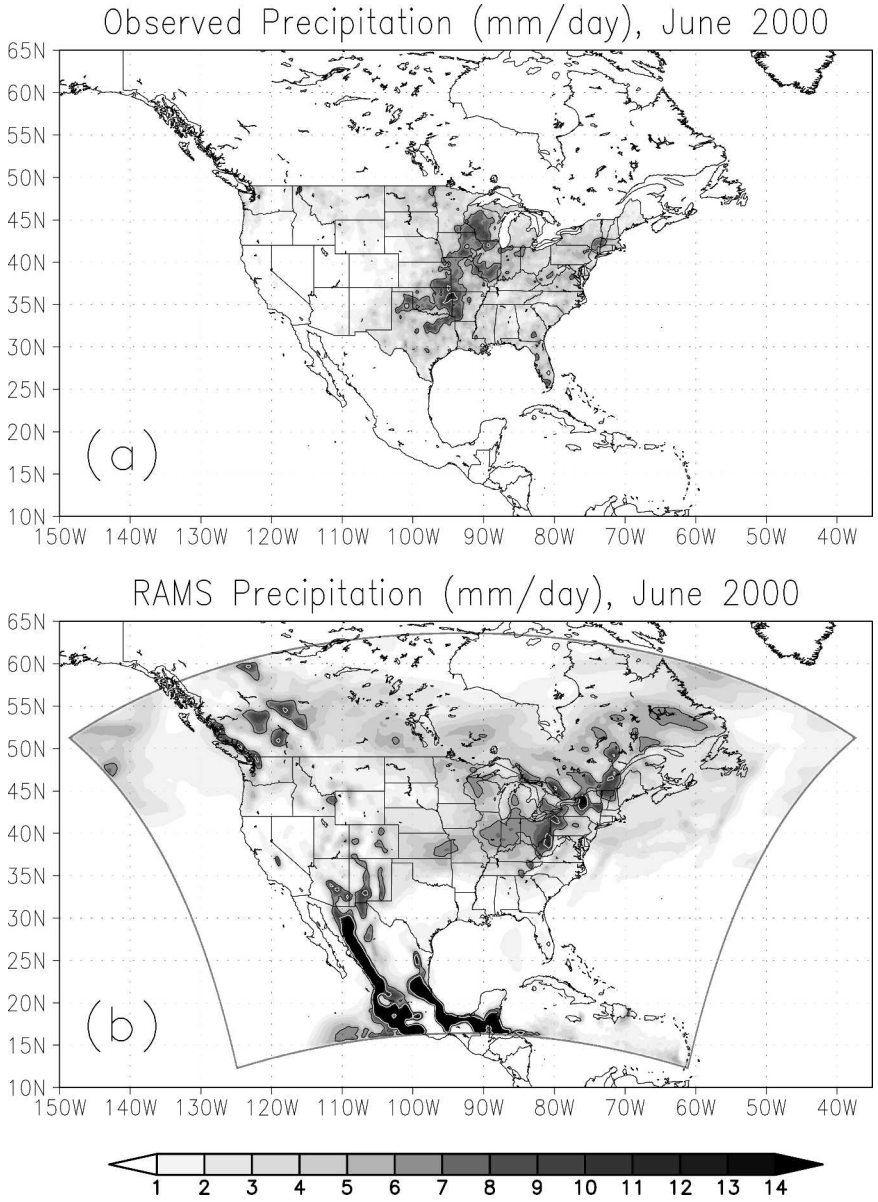

FIG. 2. Average precipitation rate for Jun 2000 (mm day^{-1}): (a) 0bservations over the United States (Reynolds et al. 2002), and (b) RAMS preliminary experiment. Contours correspond to 6 (black) and 10 mm day^{-1} (white).

is not an in-depth discussion of sensitivities, which is the subject of several studies for similar location and climatic conditions (Paegle et al. 1996; Seth and Giorgi 1998; Hong and Pan 2000; Anderson et al. 2003), but to estimate how much we can expect the results to vary by changing the surface representation and initial conditions for the soil.

4. Effects of improved resolution of surface characteristics and of soil moisture and soil temperature initialization

The mosaic approach of the LEAF-2 soil–vegetation model of RAMS allows us to increase the resolution of the soil model without changing that of the atmospheric counterpart. Grid cells are subdivided into smaller portions or "patches" corresponding to different surface characteristics occurring in the area covered by the grid cell. The extension of these patches varies depending on the relative abundance of the soil texture–vegetation class combination represented in the patch. Exchanges of water vapor, momentum, and heat occur between the atmosphere and the patches individually, and the response is area averaged for all the patches to transmit information back to the atmosphere.

We implement soil textures in the model from the Land Data Assimilation System project at 0.125° reso-

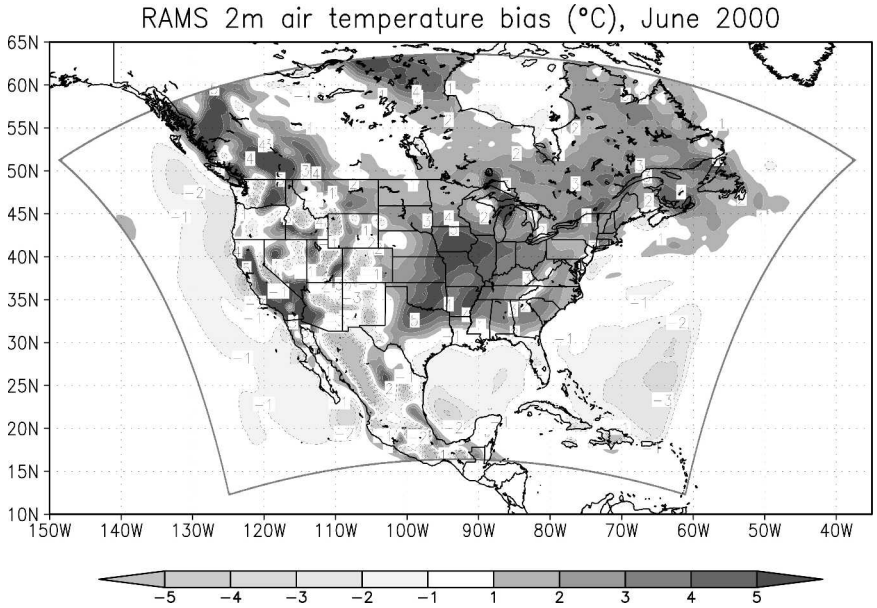

FIG. 3. Average 2-m air temperature differences for Jun 2000 (°C) between RAMS preliminary experiment and NCEP–NCAR reanalysis. Negative contours are black and dashed; positive contours are white and solid.

lution (Cosgrove et al. 2003), with 11 layers to a depth of 2.5 m, and with heterogeneity of textures in depth as well as in the horizontal. Vegetation classes and land cover are from the standard dataset in RAMS with a resolution of 0.0083°. In our experiments, we allow up to four patches per cell (plus one more when there is surface water), and therefore the soil and land cover have about 4 times more resolution than the atmospheric part of the model and the topography.

Relatively coarse resolution sea surface temperatures may not sufficiently resolve prominent features like the sharp gradient of the Gulf Stream, which is especially important for the climate of the mid-Atlantic states of the United States. In all other simulations, we utilized 4-km-resolution sea surface temperatures retrieved by the Marine Remote Sensing Laboratory of the Rutgers Institute for Marine and Coastal Sciences, in 3-day composites. These are multichannel Advanced Very High Resolution Radiometer satellite retrievals (Bernstein 1982).

Initial conditions are needed for the soil model fields, yet there are not enough routine measurements of soil variables to produce analyses similar to those of air or ocean variables. Several studies with global and regional models refer to soil moisture and its effects on climate (Beljaars et al. 1996; Paegle et al. 1996; Seth and Giorgi 1998; Hong and Pan 2000). Important quantities that define a climate, such as near-surface temperatures and precipitation, are sometimes strongly sensitive to soil moisture and soil temperature, and there is indication that the spatial distribution of soil moisture has an impact on mesoscale circulations (Georgescu et al. 2003).

The soil moisture–induced memory is much larger than that of the atmosphere, on the order of months (Delworth and Manabe 1988; Vinnikov et al. 1996; Entin et al. 2000), and for this reason initial conditions for soil moisture may have an enduring effect throughout our simulation time of 1 month. Because of this relatively long characteristic time scale, it would take a several-month-long simulation to spin up the soil model starting from an arbitrary initial condition for soil moisture and temperature (Giorgi and Mearns 1999). Furthermore, because of the strong feedbacks between atmosphere and soil, and because of deficiencies in the atmospheric model and the soil model itself, nothing guaranties that the state of the soil after the spinup simulation will come close enough to reality.

In our next experiments, we employ soil moisture and temperature from NCEP–NCAR reanalysis I (same source as initial and boundary conditions for the atmospheric part of the model) to initialize LEAF-2, the soil and vegetation model. The soil model in the reanalysis project is partially driven by observed specific humidity at the lowest atmospheric level, and it is not allowed to drift from climatology (Roads and Betts 2000). The values produced in this manner are not based on real observations of the state of the soil, but we consider that they constitute a good indication of the location of dry and wet regions (after a rain event or snowmelt) and therefore have valuable information on spatial distribution of soil moisture. NCEP–NCAR reanalysis initial soil moisture has been employed in other studies for climate simulations over North America (Takle et al. 1999; Hong and Pan 2000).

The soil moisture from NCEP–NCAR reanalysis has

only values for a top 10-cm layer and a bottom reservoir layer 2 m thick. The soil model of RAMS in our experiments has 11 layers to a depth of 2.5 m. To adapt the two-layer vertical profile from reanalysis to the RAMS multilayer soil, we adopt a simple profile where the top 10-cm value from reanalysis is assigned to all layers above a depth of 0.8 m, and a second constant value is assigned from 1-m depth to the bottom. This second constant value is such that the total amount of water in the 2-m-thick layer below 10 cm is the same as the value obtained from reanalysis. We follow this procedure, instead of just using the deep value from reanalysis from 10 cm down, because the abrupt jump in soil moisture content at 10 cm forced the top layers in RAMS to adjust very quickly, usually losing most of its water content, to a much smoother profile. Keeping the top 10-cm value constant to a depth of 0.8 m, where model soil layers are much thicker, makes this transition much slower and smoother, without significantly altering the values in the top layers, which are the ones directly interacting with the atmosphere, and preserving the information in spatial distribution of moisture content.

In the next experiment, we tried to estimate the effects of implementing heterogeneity in the soil textures, higher-resolution sea surface temperatures, and the initial soil moisture distribution based on reanalysis. Fifty-percent saturation for silty clay loam (0.232 $m^3\ m^{-3}$) means drier soil than reanalysis, which has values generally 0.05–0.10 $m^3\ m^{-3}$ higher for most of the domain, especially over northern Canada. Only on the southwestern states and northwestern Mexico, where the soil is already very dry at the beginning of June, does reanalysis have values less than 0.232 $m^3\ m^{-3}$, by about 0.10–0.15 $m^3\ m^{-3}$.

Figure 4 shows total monthly precipitation for the experiment with improved soil description and precipitation differences with the experiment with homogeneous soil textures and homogeneous soil moisture. The impact of the better description of soil properties and initial soil moisture is apparent in both panels. Large amounts of rainfall are produced in the western central Great Plains, as in the observations. However, the precipitation pattern has not changed from the preliminary experiment, and the large increase of rainfall (Fig. 4b) is clearly restricted to the tilted band across the Central Plains in a west-to-east direction. More precipitation in the west Central Plains is accompanied by significantly higher values in other areas to the east, where the observations have reduced amounts. The spatial correlation between precipitation total results from this experiment and the observations over the U.S. area east of the Rockies is, however, improved from 0.19 in the preliminary experiment to 0.34, and the root-mean-square error over the same region is now 76 versus 80 mm in the preliminary experiment.

Figure 5 shows the average 2-m air temperature differences between the experiments with improved surface characterization and initial soil moisture initialization and NCEP–NCAR reanalysis; and the differences with the experiment with homogeneous soil properties and homogeneous initial soil moisture. Biases are reduced (Fig. 5a) in comparison to the preliminary experiment (Fig. 3). Temperature differences are quite large (up to 4°C) between both experiments and are negative throughout continental areas (Fig. 5b). If we compare the average temperature differences between both experiments and the total precipitation differences (Fig. 4b), we see that the reduction of the temperature bias is not directly correlated to precipitation differences derived from the new heterogeneous initialization of soil moisture. This indicates that the large bias in near-surface temperature is not due to errors in latent heat fluxes but is mainly due to important biases in sensible heat fluxes. The reason for this can be found in the unrealistic initial soil temperatures used in the preliminary experiment, which were derived from the lowest atmospheric level, and are several degrees warmer than the soil temperatures from reanalysis. The influence of deeper soil temperatures can be different for other models, but the importance of a good initial estimate is commonly ignored in regional simulations of the order of a season, and our results show that they can be actually more influential for the near-surface temperature biases than the initial soil moisture values.

The results from the experiment described in this section indicate that a better soil moisture initialization or improvements in the land–air interaction parameterization may lead to further reduction of the model bias, especially for 2-m air temperatures. However, the precipitation differences obtained by a better representation of the soil heterogeneity and initial soil moisture and temperature conditions do not represent substantial changes in the main rainfall pattern, as shown in Fig. 4a (compared to Fig. 2b, precipitation for the preliminary experiment). This suggests that the precipitation pattern is more strongly determined by something else, at least for this nested model simulation. In the next section, we investigate the influence of the convective parameterization as we describe some modifications intended to improve observed deficiencies.

5. Effect of convective parameterization

Convective precipitation is generated in the model by a parameterization. Here we test this important component of the model in terms of its effect on precipitation amount and precipitation pattern. The standard convective parameterization in RAMS is a modified Kuo scheme. In several tests performed prior to this study, we found that the convective precipitation amounts produced with this scheme were always much smaller than observed rainfall. Grid-resolved precipitation somehow compensated for these reduced amounts so that totals were not too unrealistic. Most of the pre-

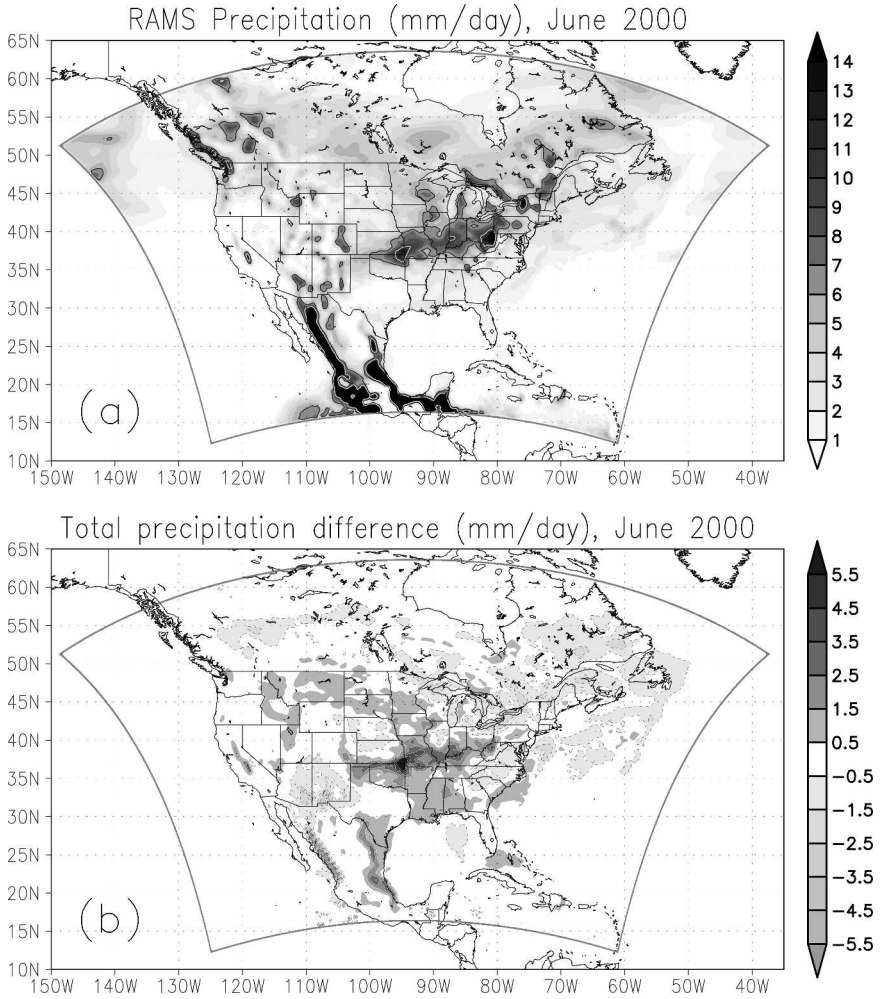

FIG. 4. Precipitation rate (mm day^{-1}) for Jun 2000 for (a) the experiment with improved surface characterization, including NCEP–NCAR reanalysis soil moisture and temperature initialization, and (b) differences (mm day^{-1}) between that experiment and the one with homogeneous soil properties, homogeneous initial soil moisture, and initial soil temperatures derived from the first atmospheric level (Fig. 2b). Contours in (a) correspond to 6 (black) and 10 mm day^{-1} (white). Negative contours in (b) are black and dashed; positive contours are white and solid.

cipitation in the case presented here is convective, and so we decided in our experiments to use a more advanced parameterization, the KF convective scheme (Kain and Fritsch 1990, 1993), which has been recently implemented in RAMS at Colorado State University, even though it is not still available in the standard release of the model. For the simulations presented in this study, most of the precipitation in the Great Plains is produced by convective parameterization when the KF scheme is used.

The Kain–Fritsch scheme is a mass flux scheme; it uses a simple cloud model to produce rearrangements of mass in the column due to subgrid convective processes. Potential updraft source layers are searched in the lowest 300 mb of the column from "parcels" 50 mb deep obtained by mixing adjacent model levels. The search starts at the surface, and each parcel is lifted undiluted to its lifted condensation level (LCL), and its thermodynamic characteristics are computed. At the LCL, a convective trigger function assigns the parcel a positive temperature perturbation based on the large-scale vertical velocity at that level. If, with this extra temperature, the parcel becomes positively buoyant, it is released from the LCL with its original temperature and an initial velocity based on its buoyancy. During the ascent, the parcel's thermodynamic characteristics and velocity are determined using a Lagrangian parcel method that considers effects of entrainment, detrainment, and water content variations (Frank and Cohen 1987). The height of the "cloud" that is formed is indicated by the level at which the velocity of the ascending parcel, now updraft, becomes negative. If the cloud

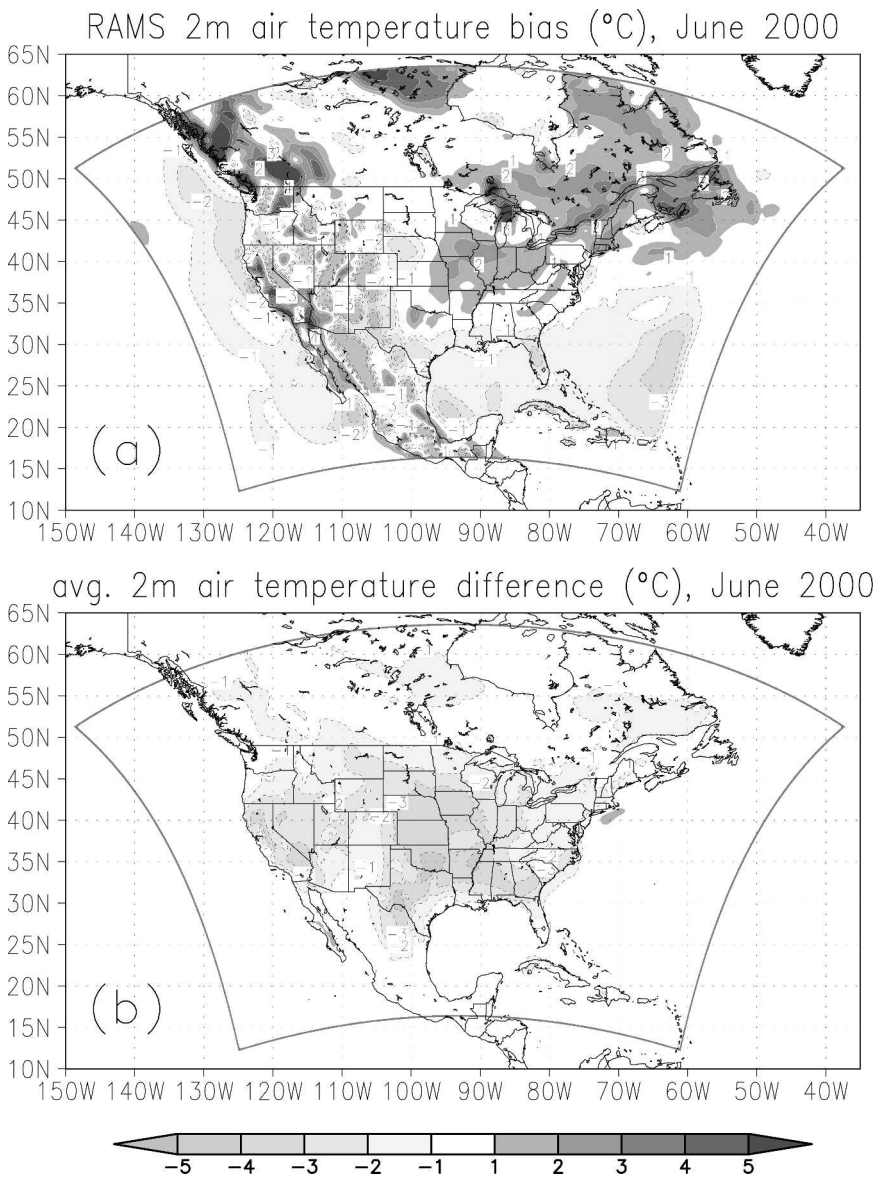

FIG. 5. Monthly average 2-m air temperature differences (°C) (a) between the experiment with improved surface characterization, including improved soil moisture and temperature initialization, and observations (NCEP–NCAR reanalysis), and (b) between the same experiment and the one with homogeneous soil properties, homogeneous initial soil moisture and initial soil temperatures derived from first atmospheric level. Negative contours are black and dashed; positive contours are white and solid.

height exceeds a threshold value, deep convection is triggered and the search for the updraft source layers stops. When deep convection has been triggered, the "unit cloud" updraft computations are completed with downdraft calculations.

The closure condition assumes that 90% of the convective available potential energy (CAPE) is removed in the column in a time span that depends on the advective time of a convective cell across the grid cell of the model, 0.5–1 h. During this time, the tendencies for temperature, moisture, and precipitation calculated from the parameterization are kept constant every time step of the integration. To fulfill the closure requirement, the mass in the column is rearranged through an iterative process where new temperature and moisture profiles are determined using the updraft and downdraft mass fluxes (entraining and detraining) from the unit cloud and the corresponding environmental fluxes necessary for mass conservation (net mass flux at any level should be zero).

A first estimate of the dependence of the precipitation patterns on the convective scheme can be ob-

tained by comparing results from the KF scheme to results from a different parameterization, such as the Kuo scheme (Kuo 1974), the scheme available in the standard release of RAMS, as mentioned previously. Figure 6 shows results from an experiment with soil improvements as described in section 3, and where the convective parameterization was changed to Kuo. The results from Kuo show less detail and diminished rainfall amounts compared with KF (Fig. 4a), however, the general pattern of a band tilted in a southwest-to-northeast direction from Oklahoma to Pennsylvania is very similar in both simulations. Observations (Fig. 2a) show the precipitation directed more in a south-to-north direction across the central plains and much more reduced in the rest of the United States.

The triggering mechanism for convection in the Kuo scheme is based upon low-level convergence, given by the large-scale vertical velocity at the LCL. Vertical velocity (w) also plays a role in the activation of the KF scheme, since the parcels are given a perturbation temperature dependent on the vertical velocity at the LCL. Moreover, the radius of the unit cloud, which determines the maximum possible entrainment rate, also depends on w. Nevertheless, the precipitation pattern is not entirely justified by this common dependence on w, since in the KF scheme there are more elements that play an important role in triggering convection. Because of the complexity of the scheme, one question that arises is whether the results depend mostly on the assumptions used in the triggering function, unit cloud calculations, or the closure condition.

Since the intensity of the convection depends explicitly on CAPE in the KF scheme, one would expect that there should be some sort of relationship between CAPE, precipitation, and frequency of activation of the parameterization. Figure 7 shows the average CAPE per convective event, the number of convective events per day, and total precipitation from the convective parameterization. "Convective event" means every occasion that the convective scheme has been called with result of deep convection activated (with convective tendencies to be applied as constant for 1 h, as discussed previously). Panels in the left column are for the simulation with the original KF scheme. Most of the precipitation during this month is produced by the convective parameterization, at least over the United States (cf. Fig. 7c with Fig. 4a). It also seems that deep convection is triggered at an unreasonably high frequency over many areas (Fig. 7b) and that most of those events are produced with relatively small CAPE (less than 300 $m^2 s^{-2}$). This is partially due to the lower threshold cloud depth needed to produce deep convection for colder environments. The average CAPE per event (Fig. 7a) does not relate well to the total precipitation (Fig. 7c).

According to the results reflected in the left column of Fig. 7, events with small CAPE and low rainfall (the average rainfall per convective event pattern matches nicely the average CAPE per event pattern; not shown) are more abundant than they should be in several areas and may create the observed bias in the total precipitation pattern. To try to correct this, we introduce probability in the triggering of deep convection using a ran-

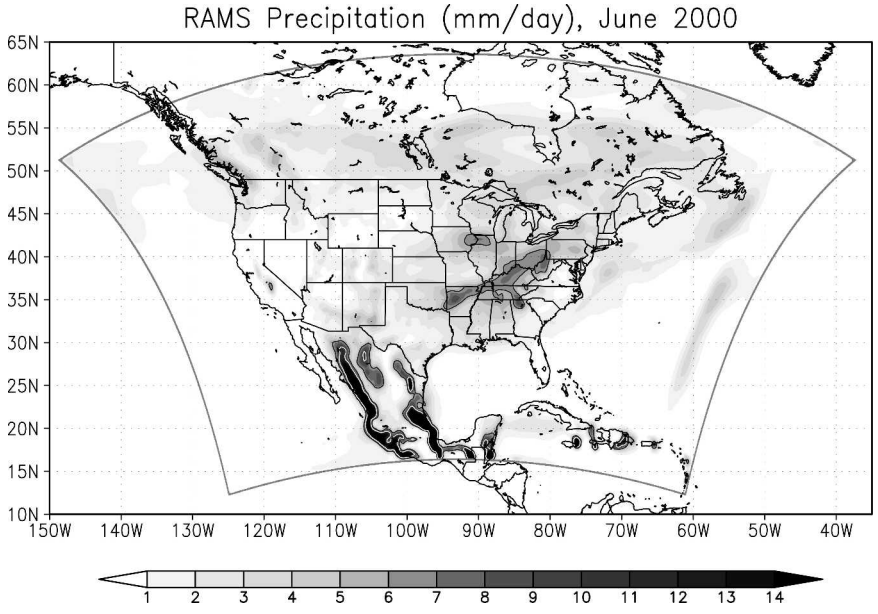

FIG. 6. Average precipitation rate (mm day^{-1}) for Jun 2000 for the experiment with improved soil representation and initialization and Kuo convective scheme. Contours correspond to 6 (black) and 10 mm day^{-1} (white).

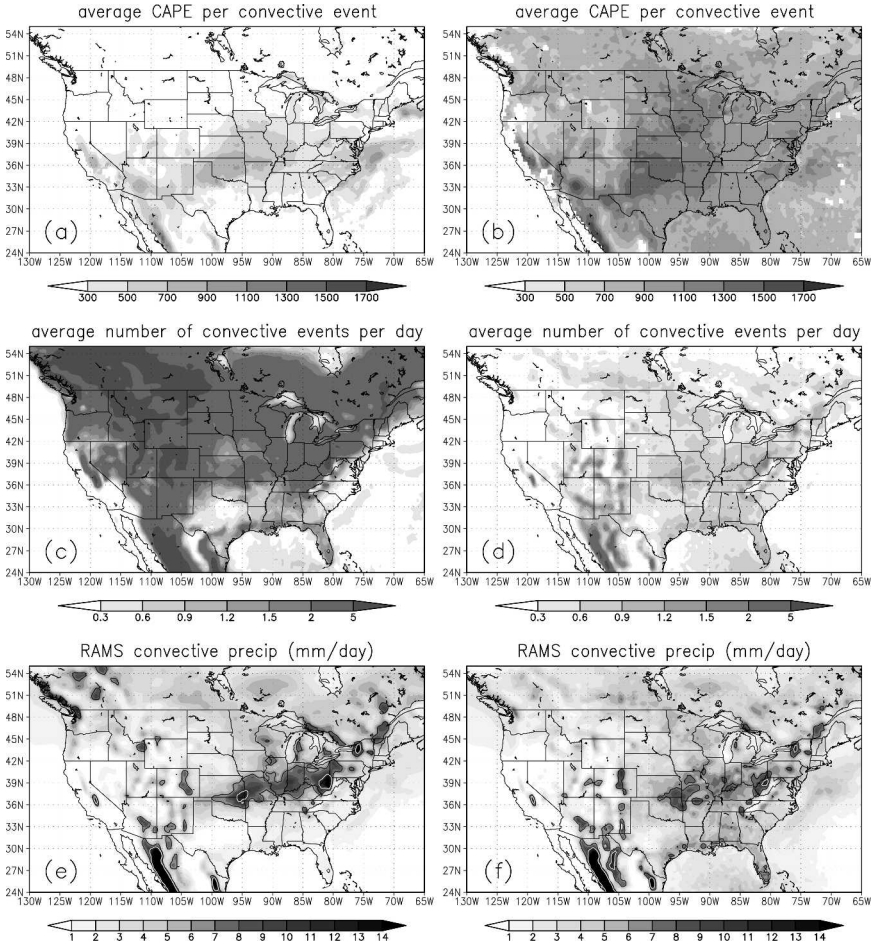

FIG. 7. (a), (b) Average CAPE ($m^2 s^{-2}$) per convective event; (c), (d) average number of convective events per day; and (e), (f) average monthly convective precipitation (mm day^{-1}), (left) for the experiment with the original KF scheme and (right) for the experiment with the modified (see text) KF scheme. Contours in (e) and (f) correspond to 6 (black) and 10 mm day^{-1}(white).

dom number generator with a probability function depending on CAPE. The probability distribution follows a cubic function of CAPE. For CAPE < 200 $m^2 s^{-2}$ in a column, the probability is 0, and it is 1 for CAPE $>$ 1500 $m^2 s^{-2}$. With this modification, even if all conditions in the convective scheme for a parcel to trigger deep convection are satisfied, if the value of CAPE is close to 200 $m^2 s^{-2}$, deep convection is unlikely to occur. If convection is not triggered, the search for the updraft source layer is not ended but moved up one level, so there are other chances for deep convection to be triggered in the same time step for the same column. Most likely, shallow convection (which is also handled by the parameterization) or no convection is triggered instead, since parcels farther up from the surface tend to be more stable.

Other attempts that we have made to promote high CAPE events, which on the other hand are already favored to produce convection and precipitation, include introducing a dependence of the radius of the unit cloud on CAPE and not only on vertical velocity at the LCL. In this way, situations with small large-scale convergence but a reasonable amount of CAPE are made more likely to trigger convection. The effect of that change is only important in the south of our domain (in the Gulf of Mexico area), where large-scale convergence is small (Fig. 7f).

The right column of Fig. 7 shows results after the aforementioned modifications in the KF scheme have been introduced. If we compare Figs. 7b and 7e, we observe that convective events are drastically reduced over Canada with the introduction of the probabilistic trigger, but comparing Figs. 7c and 7f for total convective precipitation, we see that the precipitation pattern and amounts are not affected so dramatically. Moreover, the precipitation pattern and the pattern of the number of convective events now show a very clear correspondence. The average CAPE per convective

event (Fig. 7d) shows a very good pattern similarity with the observed precipitation (Fig. 2a).

Interpretation of these results is not straightforward. On one hand, the simulated average CAPE has a distribution consistent with the observed precipitation, but on the other hand, simulated convective precipitation does not, and the erroneous rainfall pattern is mostly due to convective events triggered with a small amount of CAPE. In a test (not shown) where all dependence on w (large-scale convergence) was removed from the KF scheme, results were surprisingly very similar. Therefore, there must be another element implicit in the convective calculations that actually plays the predominant role in triggering and modulating convective precipitation. Some studies have suggested that this element is midtropospheric moisture (Shepherd et al. 2001), which is advected by the dynamics and not generated locally by evaporation. This would be consistent with the fact that modifying the convective scheme or using a different one did not change the large-scale rainfall pattern substantially and points at a dynamical bias and not directly to the convective scheme as the reason the discrepancy with observations.

In Fig. 8, we show monthly average precipitation after the modifications of the KF scheme have been introduced and precipitation differences with the experiment with the original KF scheme. Overall the total precipitation looks more realistic and closer to observations (Fig. 2a), especially over areas in the proximity of the Gulf of Mexico, which were completely dry before. However, as mentioned before, the main pattern has not changed for the most part (the spatial correlation of precipitation totals from this experiment and observations for the United States east of the Rockies is now 0.34, exactly the same as in the previous experi-

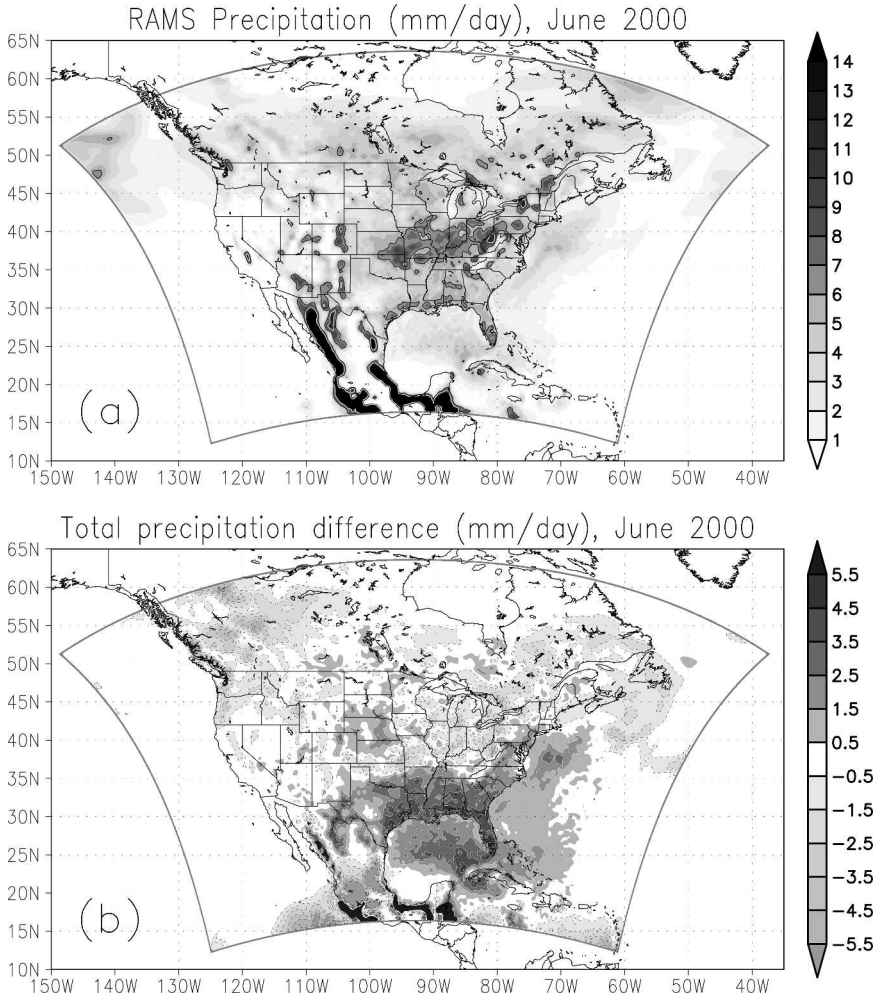

FIG. 8. Total monthly precipitation (mm day^{-1}) for (a) the experiment with the modified KF scheme and (b) precipitation differences (mm day^{-1}) between the same experiment and the one with the original KF scheme. Contours in (a) correspond to 6 (black) and 10 mm day^{-1} (white). Negative contours in (b) are black and dashed; positive contours are white and solid.

ment with unchanged convective scheme), even though as we see in the differences with the experiment with the original KF scheme, there has been a diminution of the rainfall total along the band across the central United States, and the precipitation has been redistributed to other areas. The root-mean-square error of the precipitation totals has decreased about 20% with the changes in the convective scheme, from 76 to 61 mm. Air temperature biases, shown in Fig. 9, are slightly reduced from what they were before we performed the changes in the convective scheme (Fig. 6b) and are more affected by modifications in the soil initialization.

The experiments that we have described in this section, where we compare the KF scheme with the Kuo scheme or modify the KF scheme, show that even though the precipitation amounts do respond to the change or the "tuning" of the parameterization, the precipitation pattern seems to be more determined by some other factors, very likely related to errors in the dynamics. In the next section, we investigate this possibility.

6. Boundary and dynamical effects: Spectral nudging

We now examine the tropospheric circulation and how the biases observed in the precipitation patterns are related to anomalies in the dynamic fields. Figure 10 shows 200-mb zonal and meridional wind average differences between the simulation with the improved model and NCEP–NCAR reanalysis. The biases in the circulation present a longwave pattern, produced by phase shifts or oscillations in the amplitude of the waves in the circulation. Results for other levels also exhibit a similar structure.

One plausible explanation for the wavelike anomalies observed in the upper-tropospheric wind (Fig. 10) has to do with the lateral boundaries. Since wavenumbers 1 and 2 can interact with the boundaries practically from each internal location in the domain, their amplitudes and phases depend on the position of the domain borders and boundary conditions. It is known that errors associated with advective transport accumulate at the "exit" boundaries, as a result of inconsistencies between the model solution and the boundary conditions caused by overspecification (boundary conditions are not really needed for the exit boundaries; see, e.g., Staniforth 1997). The impact of such inconsistencies for short-term integrations remains in the regions close to the boundaries; however, for a longer integration like in our experiments, this appears not to be the case. Errors accumulate in the boundary regions. They are too far to be removed by the boundary nudging and therefore propagate back and interfere with the circulation creating the average bias with the wave pattern that we see in Fig. 10. The circulation bias in the model is therefore not directly related to local misrepresentation of physical processes like convection or land–air interaction but is defined by a combination of errors from all processes throughout the domain that propagate, accumulate, and reflect in the boundaries

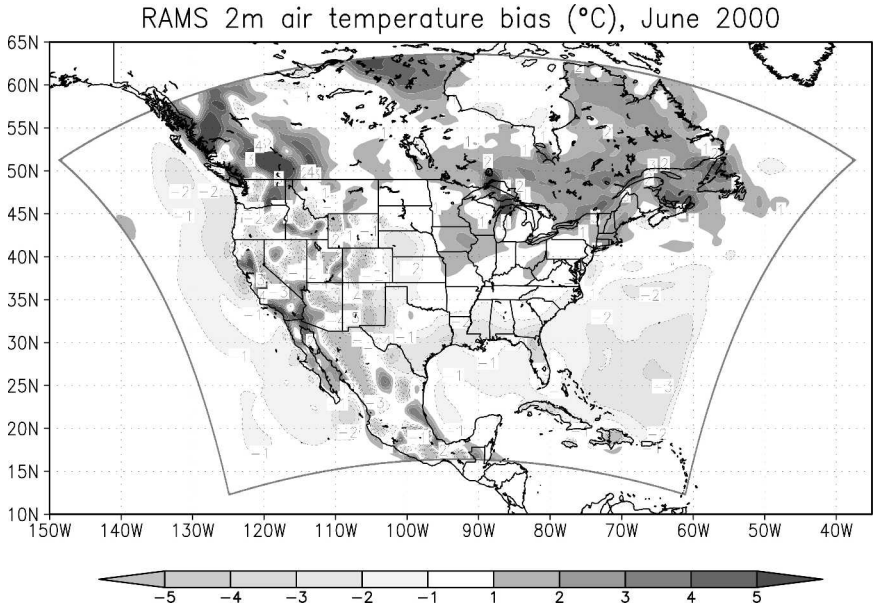

FIG. 9. Monthly average 2-m air temperature differences (°C) between the experiment with improved surface characterization, including soil moisture and temperature initialization and modified KF convective scheme, and NCEP–NCAR reanalysis. Negative contours are black and dashed; positive contours are white and solid.

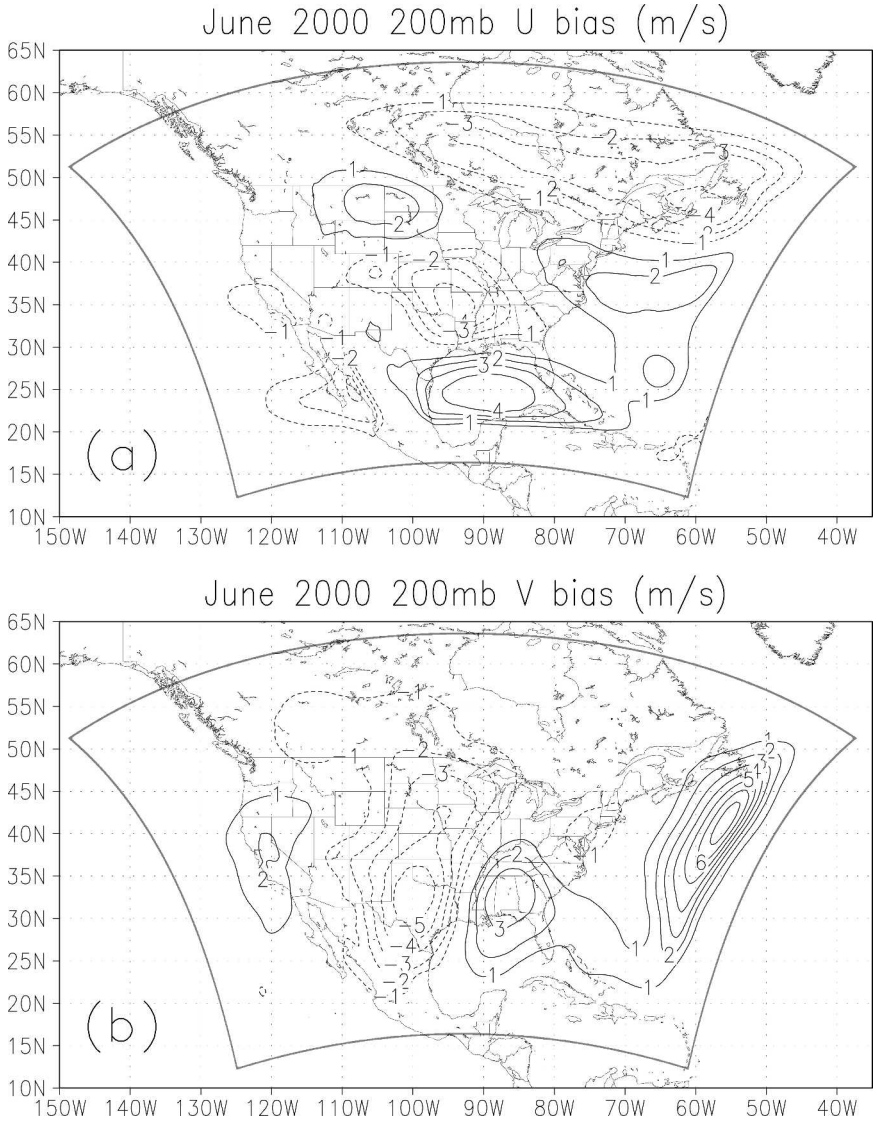

FIG. 10. Monthly average differences between RAMS experiment and NCEP/NCAR reanalysis at 200 mb for (a) u (m s^{-1}) and (b) v (m s^{-1}). Contour interval is 1 m s^{-1} and negative contours are dashed.

contaminating the model's solution throughout domain.

In our case, the circulation parallel to the Rocky Mountains, including the low-level jet that plays a key role in the precipitation pattern on the Great Plains, seems to be particularly affected by the background bias due to the presence of the "wall" boundary on the west. Figure 11 illustrates average differences between RAMS and reanalysis for 850-mb u, v, and geopotential heights. During this month, there is a relatively strong zonal circulation across the north of our domain, while we have easterlies in the southern boundary. In between the circulation is not so strong, certainly not enough to remove errors at the boundary, which instead accumulate and reflect, altering the large-scale flow in the whole domain. Figure 11c shows a large bias in geopotential heights close to the western boundary, with another one of about the same size over the Rockies (even though because of interpolation discrepancies due to topography differences between RAMS and reanalysis, the bias over the mountains does not show as cleanly at this 850-mb level as it does over flat terrain). This error pattern is clearly not due to local processes. As a consequence of the erroneous mass fields, the circulation is affected, and the flow of moisture from the Gulf of Mexico into the Great Plains in our simulations has on average a weaker meridional component (about 3 m s^{-1} less) than reanalysis (Fig. 11b), veering to the east across the central Plains, instead of following a more south-to-north path. The bias

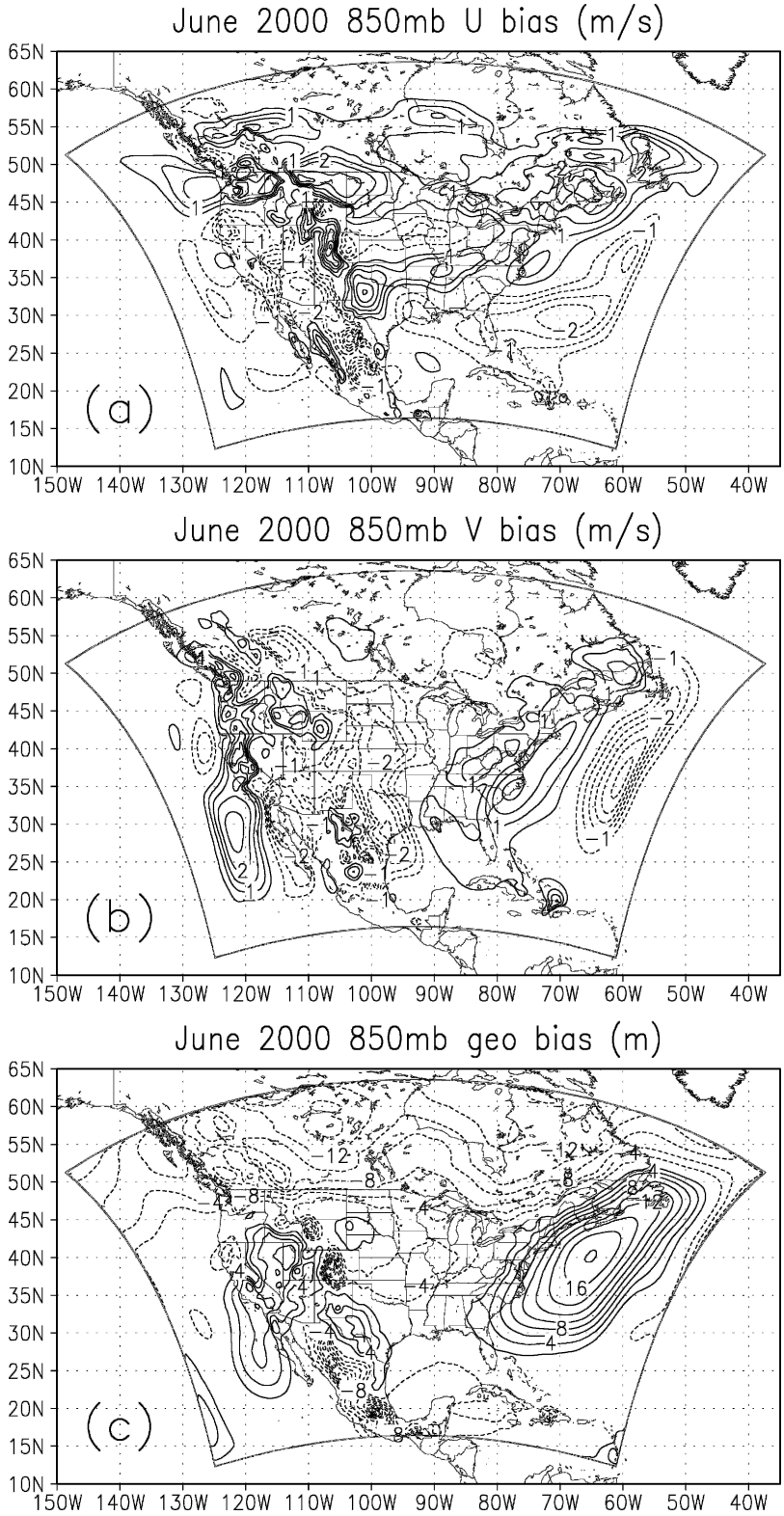

FIG. 11. Monthly average differences between RAMS experiment and NCEP–NCAR reanalysis at 850 mb for (a) u (m s^{-1}), (b) v (m s^{-1}), and (c) geopotential height (m). Contour interval is 0.5 m s^{-1} in (a) and (b) and 2 m in (c), and negative contours are dashed.

in the u wind at this 850-mb level (Fig. 11a) also shows the wave disposition, which is organized by the Rocky Mountains with maxima and minima aligned downstream from the mountain chain. It is likely that for other regions of the world, seasons, and domain sizes, the bias inherent to the chosen domain geometry would be different.

The interference in the dynamics due to the presence of the boundaries can also affect sensitivities in the model, especially for precipitation. Figure 12 shows differences in the 200-mb u and v components of the wind between the experiment with the improved surface and initial soil conditions from NCEP–NCAR reanalysis, and the preliminary experiment, with homogeneous soil and soil moisture. The differences also exhibit a long wave pattern that indicates control from the lateral boundaries even in the center of the domain.

To test the hypothesis that the large-scale dynamics are altered by the lateral boundary effects described above, we implemented a spectral nudging technique in RAMS to control the amplitudes and phases of waves with small wave numbers (Waldron et al. 1996; von Storch et al. 2000). In spectral nudging, a new term is added to the tendencies that relaxes the selected part of the spectrum to the corresponding waves from reanalysis:

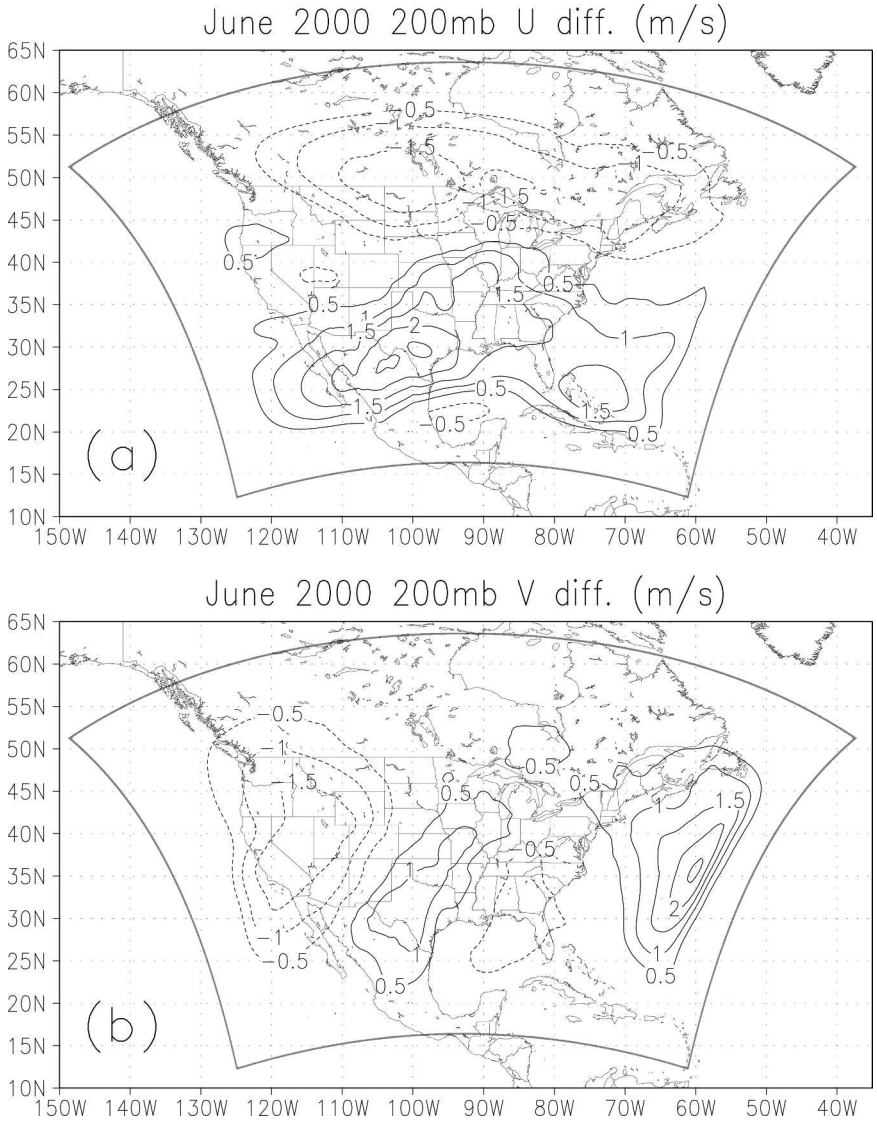

FIG. 12. (a) Monthly average differences in 200-mb u wind (m s^{-1}) between RAMS experiment with improved soil and initial soil moisture and temperatures from NCEP–NCAR reanalysis and the experiment with homogeneous soil textures and homogeneous initial soil moisture. (b) Same as in (a), but for the v component of the wind. Contour interval is 1 m s^{-1} and negative contours are dashed.

$$\frac{dQ}{dt} = L(Q) - \sum_{|n|\le N} \sum_{|m|\le M} K_{mn}(Q_{mn} - Q_{omn})e^{ik_m x} e^{ik_n y},$$

where Q is any of the prognostic variables to nudge, L is the model operator, and Q_o is the reanalysis variable. Here, Q_{mn} and Q_{omn} are the spectral coefficients of Q and Q_o, respectively, and K_{mn} is the nudging coefficient, which can vary with m and n and also with height.

The relaxation term, with only the coefficients for the selected part of the spectrum, is transformed from wave space to physical space and added to the tendency for the prognosed variable Q. Because of the orthogonality of the functions of the Fourier expansion, only the same part of the spectrum of variable Q will be affected by the relaxation.

To calculate the strength of the nudging at every point, we decompose in Fourier series the difference fields $Q - Q_o$ (model minus reanalysis) to calculate the spectral coefficients and filter out the short waves. The nudging applied in the buffer zone at the edges of the domain diminishes the values of $Q - Q_o$ at the boundaries, which makes these difference fields quasi-periodic and reduces errors in the Fourier decomposition. RAMS is executed in parallel on separate computer nodes, and this poses an added difficulty for the procedure, since values for the whole domain are necessary to perform the spectral decomposition. The communication with the master node required to gather fields from the nodes in order to carry out the decomposition slows the integration quite a bit, and so it only takes place every third time step. The spectral nudging occurs with that frequency.

We perform an experiment where nudging is applied for wavenumbers 0, 1, 2, and 3 in the x direction and 0, 1, and 2 in the y direction (for this domain size, this means wavelengths of about 2500 km) and for variables u, v, θ_{il}, and π' (winds, potential temperature ice–liquid, and perturbation Exner function). We choose not to nudge moisture fields because their variations in the horizontal, and especially in the vertical, can be very pronounced and likely to be missed by coarse resolution reanalyses. The strength of the nudging depends on coefficient K_{mn}, which is set to be a function of height, being zero in the boundary layer and increasing smoothly from about 1500 m above the terrain to become constant in the upper troposphere with a characteristic time for the relaxation of 5000 s.

Figure 13a shows total precipitation results for the simulation where the large-scale circulation is relaxed to reanalysis, and Fig. 13b shows total precipitation differences with the experiment with no spectral nudging. Results are improved substantially with more rainfall in the northern Great Plains and less in the southeast of the United States (cf. also to observations in Fig. 2a), and they also exhibit small-scale structure, which was the main reason to nest the regional model in the first place, since the model is still unconstrained to develop wavenumbers higher than 2. The spatial correlation between the precipitation totals from this experiment in the U.S. area east of the Rockies and the observations is now 0.45, whereas it was 0.34 for the previous experiment with the same model setup but no spectral nudging. The root-mean-square errors have also been reduced from 61 to 55 mm. There are still important small-scale precipitation errors in mountainous areas of the West, however. We have indications that these large precipitation values in the steep slopes are due to the relatively large horizontal diffusion required for numerical stability, which is applied on sigma surfaces, and there is not an easy fix for this problem.

Correcting only long waves is sufficient to eliminate the mid- and upper-tropospheric circulation biases (not shown) and substantially improve precipitation results, both in amount and pattern (without any nudging being applied to moisture) and supports the conjecture that the precipitation biases are caused by recurrent distortions in the large-scale circulation due to the presence of the lateral boundaries.

It is important that nudging be performed in the entire free troposphere above the top of the boundary layer. A test (not shown) indicated that nudging of the upper-tropospheric circulation (above 6000 m) alone was not enough to alter the erroneous precipitation pattern. We do not have a clear answer as to why a correct circulation in the upper troposphere was not sufficient to keep the large-scale lower-tropospheric circulation close to observations. Perhaps some other factors, like the interaction with the mountains that occurs at lower levels, are more important, and the nudging needs to be deeper down to lower levels to prevent the boundary effects previously discussed.

7. Discussion and conclusions

It is well known that a regional climate model can produce significantly different results before and after a careful evaluation against observations is performed and corrective measures for errors are applied. In this study, we investigate the reasons for biases in regional climate simulations, trying to discern whether they arise from deficiencies in the model parameterizations or are due to dynamical problems. The regional model utilized is RAMS, which we adapt for large domains by considering terms in the equations that were previously neglected. In addition, the turbulent parameterization was corrected, so that derived vertical mixing coefficients cannot attain the unrealistically high values that appeared mostly in the midtroposphere from problems in the Mellor–Yamada turbulence parameterization.

We performed model integrations for summer climate over North America, and preliminary experiments showed large biases in precipitation and near-surface temperatures. For summer climate for this region, two key factors are land–air interaction and convection, and for this reason we examined the effect

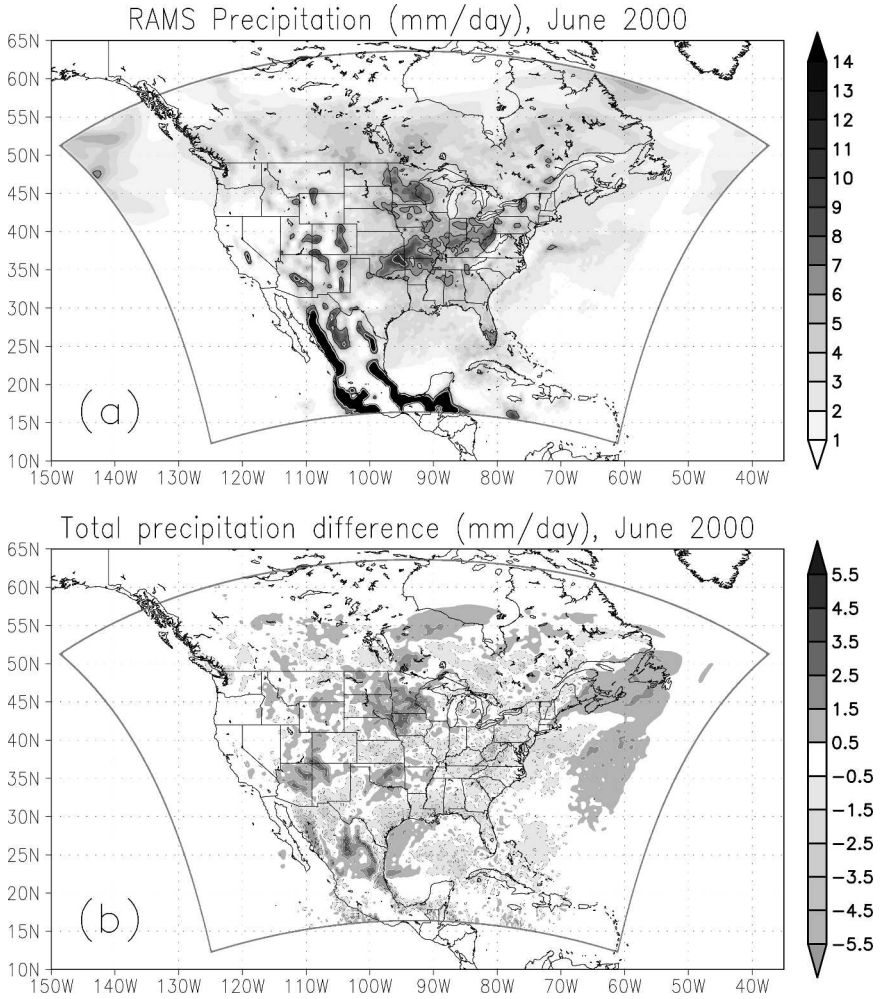

FIG. 13. (a) Average monthly precipitation (mm day^{-1}) for the experiment with spectral nudging and (b) precipitation differences (mm day^{-1}) between the same experiment and the one without spectral nudging. Contours in (a) correspond to 6 (black) and 10 mm day^{-1} (white). Negative contours in (b) are black and dashed; positive contours are white and solid.

on the results of improvements in the parameterizations of those processes. First we implemented high-resolution soil textures and SSTs and initialized soil moisture and temperatures from NCEP–NCAR reanalysis, and then we examined the impact of modifications in the Kain–Fritsch convective parameterization. Our results indicate that near-surface temperatures respond readily to changes in the surface conditions, including soil moisture and temperature. In addition, they also respond to cloudiness. For precipitation, amounts vary in certain areas because of different initial soil moisture and temperature conditions, soil property representation, or "tunings" in the convective parameterization. These conclusions agree with what has been reported in other studies (Seth and Giorgi 1998; Takle et al. 1999; Hong and Pan 2000; Anderson et al. 2003). We observe, however, that there are some common features in the model bias, especially in the erroneous precipitation pattern, that are related to dynamical processes rather than directly to model deficiencies. Dynamical deficiencies in the nested model have previously been assigned to errors in the boundary conditions, especially when the data at the boundaries are from a GCM (e.g., Noguer et al. 1998). In our case, we utilize NCEP–NCAR reanalysis as driving fields, and therefore the possibility that they are the source for the dynamical bias can be discarded, since North America is an area of high density in the observational network.

An examination of the average circulation errors in our simulations shows that they organize in a long wave pattern and that error values are largest close to the "exit" boundaries, where boundary conditions are actually overspecified (Staniforth 1997). The cause of the long wave organization of circulation biases is the accumulation of errors near the lateral boundaries and

TABLE 1. Spatial correlations with observed precipitation and rms errors of precipitation for the month of Jun 2000 for the region between 20° and 48°N and 100° and 75°W (the United States east of the Rockies) for the four different experiments described in the text.

	Preliminary	Improved surface	Also improved convection	Also spectral nudging
Spatial correlation	0.19	0.34	0.34	0.45
Rms error (mm)	81	76	66	55

their back reflection due to the artificial constraint that the boundary conditions pose. The particular pattern depends on the geometry and location of the grid and on the circulation going through it. This dependence on the domain geometry explains findings in other studies, like high sensitivity to domain size (Seth and Giorgi 1998) and similarities in precipitation biases between very different RCMs that use a similar model grid (Anderson et al. 2003).

For our simulations over North America, the domain is crossed by the Rocky Mountains, which generate and intensify waves in the circulation that significantly alters the flow entering through the western boundary. Errors produced in the interior of the domain reflect in the lateral boundaries and interfere with the dynamics modifying the meridional circulation on the lee of the Rocky Mountains, including the low-level jet, weakening the south-to-north flow that transports the moisture from the Gulf of Mexico into the Northern Great Plains. The precipitation pattern is affected and becomes significantly more zonal, a configuration that we are not able to alter substantially by changes in the model parameterizations. Model sensitivities are also affected by this problem, since the enclosed domain forces perturbations to organize in long wave patterns.

As a plausible solution for the boundary reflection problem, we introduced spectral nudging into RAMS, in which the long waves of the model variables (except moisture) are relaxed to the long waves of reanalysis at all levels above the boundary layer and throughout the domain. Relaxation of waves 0, 1, and 2 in the y direction and of 0, 1, 2, and 3 in the x direction (about 2500-km wavelength) above the boundary layer is sufficient to eliminate the bias in the circulation and to produce a much-improved precipitation pattern, maintaining the development of the small-scale structure that was the reason for nesting the regional model in the first place. Since these long waves are supposed to be determined by the boundary conditions (they are well within the reanalysis resolution), and are not to be significantly changed by the model, this relaxation of the long waves to the driving fields might be necessary when using regional models in climate mode.

Table 1 summarizes the improvement of precipitation total results in the successive experiments discussed above. We also found that 2-m air temperatures biases can be largely reduced by improvements in the representation of the surface, such as high-resolution soil texture and sea surface temperatures, together with a heterogeneous initialization of soil moisture and temperature from NCEP–NCAR reanalysis (even though these soil data are only inferred from previously observed weather). Total monthly precipitation amounts also respond to a different initial state of the soil and surface description. However, the sensitivity is weaker than for 2-m air temperatures. While near-surface temperatures respond to changes in the soil throughout the land areas of the domain, precipitation is redistributed following mostly the original erroneous pattern. The bias is related to convective events with low CAPE triggered in the band oriented east–west along the central United States, following the path of midtropospheric advected moisture, and by a diminution of convective events in the Northern Great Plains and Texas. The reason for this is not directly related to the convective scheme, since the pattern could not be altered by significant modifications in the Kain–Fritsch convective scheme or by replacing it with the Kuo scheme.

These conclusions are illustrated by the detailed example for June 2000. However, we have repeated this study for other summer months, and other years receive the same conclusions. The precipitation patterns are different for each case, as they depend on the large-scale circulation, but spectral nudging is required for good climate simulations. We also expect these results to be applicable to other regional climate models and not to be specific to RAMS.

Acknowledgments. We thank Chris Castro and Adriana Beltran for providing us with the Kain–Fritsch convective parameterization. We also thank Chris Weaver, Jan Paegle, and Bob Walko for valuable comments on the work. NCEP–NCAR reanalysis data and Reynolds SST data were provided by the NOAA–CIRES Climate Diagnostics Center, Boulder, Colorado (http://www.cdc.noaa.gov/). This paper was supported by the Center for Environmental Prediction, Cook College, NASA Goddard Institute for Space Sciences Grant NCC5-553, and New Jersey Department of Environmental Protection Contracts SR-00-048 and SR-02-082.

REFERENCES

Anderson, C. J., and Coauthors, 2003: Hydrological processes in regional climate model simulations of the central United States flood of June–July 1993. *J. Hydrometeor.,* **4,** 584–598.

Beljaars, A. C. M., P. Viterbo, M. J. Miller, and A. K. Betts, 1996: The anomalous rainfall over the United States during July 1993: Sensitivity to land surface parameterization and soil moisture anomalies. *Mon. Wea. Rev.,* **124,** 362–383.

Bernstein, R. L., 1982: Sea surface temperature estimation using

the NOAA-6 advanced very high resolution radiometer. *J. Geophys. Res.,* **87,** 9455–9465.

Christensen, J. H., B. Machenhauer, R. G. Jones, C. Schär, P. M. Ruti, M. Castro, and G. Visconti, 1997: Validation of present-day regional climate simulations over Europe: LAM simulations with observed boundary conditions. *Climate Dyn.,* **13,** 489–506.

Cosgrove, B. A., and Coauthors, 2003: Real-time and retrospective forcing in the North American Land Data Assimilation Systems (NLDAS) project. *J. Geophys. Res.,* **108,** 8842, doi:10.1029/2002JD003118.

Cotton, R. W., and Coauthors, 2003: RAMS 2001: Current status and future directions. *Meteor. Atmos. Phys.,* **82,** 5–29.

Delworth, T., and S. Manabe, 1988: The influence of potential evaporation on the variabilities of simulated soil wetness and climate. *J. Climate,* **1,** 523–547.

Denis, B., R. Laprise, D. Caya, and J. Coté, 2002: Downscaling ability of one-way nested regional climate models: The Big-Brother Experiment. *Climate Dyn.,* **18,** 627–646.

Dickinson, R. E., R. M. Errico, F. Giorgi, and G. T. Bates, 1989: A regional climate model for the western United States. *Climate Change,* **15,** 383–422.

Entin, J. K., A. Robock, K. Y. Vinnikov, S. E. Hollinger, S. Liu, and A. Namkhai, 2000: Temporal and spatial scales of observed soil moisture variations in the extratropics. *J. Geophys. Res.,* **105,** 11 865–11 877.

Fox-Rabinovitz, M., G. L. Stenchikov, M. J. Suarez, L. L. Takacs, and R. C. Govindaraju, 2000: A uniform- and variable-resolution stretched-grid GCM dynamical core with realistic orography. *Mon. Wea. Rev.,* **128,** 1883–1898.

Frank, W. M., and C. Cohen, 1987: Simulation of tropical convective systems. Part I: A cumulus parameterization. *J. Atmos. Sci.,* **44,** 3787–3799.

Frei, C., J. H. Christensen, M. Déqué, D. Jacob, R. G. Jones, and P. L. Vidale, 2003: Daily precipitation statistics in regional climate models: Evaluation and intercomparison for the European Alps. *J. Geophys. Res.,* **108,** 4124, doi:10.1029/2002JD002287.

Gal-Chen, T., and R. C. J. Somerville, 1975: On the use of coordinate transformation for the solution of the Navier-Stokes equations. *J. Comput. Phys.,* **17,** 209–228.

Georgescu, M., C. P. Weaver, R. Avissar, R. L. Walko, and G. Miguez-Macho, 2003: Sensitivity of model-simulated summertime precipitation over the Mississippi River basin to spatial distribution of initial soil moisture. *J. Geophys. Res.,* **108,** 8855, doi:10.1029/2002JD003107.

Giorgi, F., 1990: Simulation of regional climate using a limited area model nested in a general circulation model. *J. Climate,* **3,** 941–963.

——, and L. O. Mearns, 1999: Introduction to special section: Regional climate modeling revisited. *J. Geophys. Res.,* **104** (D6), 6335–6352.

Harrington, J. Y., 1997: The effects of radiative and microphysical processes on simulated warm and transition season arctic stratus. Ph.D. dissertation, Atmospheric Science Paper 637, Colorado State University, 289 pp.

Higgins, R. W., W. Shi, E. Yarosh, and R. Joyce, 2000: *Improved US Precipitation Quality Control System and Analysis*. NCEP/Climate Prediction Center Atlas 7, National Centers for Environmental Prediction, Washington, DC, 40 pp.

Hong, S.-Y., and A. Leetmaa, 1999: An evaluation of the NCEP RSM for regional climate modeling. *J. Climate,* **12,** 592–609.

——, and H.-L. Pan, 2000: Impact of soil moisture anomalies on seasonal summertime circulation over North America in a regional climate model. *J. Geophys. Res.,* **105** (D24), 29 625–29 634.

Kain, J. S., and J. M. Fritsch, 1990: A one-dimensional entraining/detraining plume model and its application in convective parameterization. *J. Atmos. Sci.,* **47,** 1890–1910.

——, and ——, 1993: Convective parameterization for mesoscale models: The Kain–Fritsch scheme. *The Representation of Cumulus Convection in Numerical Models, Meteor. Monogr.*, No. 46, Amer. Meteor. Soc., 165–170.

Kalnay, E., and Coauthors, 1996: The NCEP/NCAR 40-Year Reanalysis Project. *Bull. Amer. Meteor. Soc.,* **77,** 437–471.

Kuo, H. L., 1974: Further studies of the parameterization of the influence of cumulus convection on large-scale flow. *J. Atmos. Sci.,* **31,** 1232–1240.

Liang, X.-Z., K. E. Kunkel, and A. N. Samel, 2001: Development of a regional climate model for U.S. Midwest applications. Part I: Sensitivity to buffer zone treatment. *J. Climate,* **14,** 4363–4378.

Liston, G. E., and R. A. Pielke Sr., 2000: A climate version of the regional atmospheric modeling system. *Theor. Appl. Climatol.,* **66,** 29–47.

Mellor, G. L., and T. Yamada, 1974: A hierarchy of turbulence closure models for planetary boundary layers. *J. Atmos. Sci.,* **31,** 1791–1806.

Miguez-Macho, G., G. L. Stenchikov, and A. Robock, 2004: Spectral nudging to eliminate the effects of domain position and geometry in regional climate model simulations. *J. Geophys. Res.,* **109,** D13104, doi:10.1029/2003JD004495.

Noguer, M., R. Jones, and J. Murphy, 1998: Sources of systematic errors in the climatology of a regional climate model over Europe. *Climate Dyn.,* **14,** 691–712.

Paegle, J., K. C. Mo, and J. Nogués-Paegle, 1996: Dependence of simulated precipitation on surface evaporation during the 1993 United States summer floods. *Mon. Wea. Rev.,* **124,** 345–361.

Pielke, R. A., and Coauthors, 1992: A comprehensive meteorological modeling system—RAMS. *Meteor. Atmos. Phys.,* **49,** 65–78.

Reynolds, R. W., N. A. Rayner, T. M. Smith, D. C. Stokes, and W. Wang, 2002: An improved in situ and satellite SST analysis for climate. *J. Climate,* **15,** 1609–1625.

Roads, J., and A. Betts, 2000: NCEP–NCAR and ECMWF reanalysis surface water and energy budgets for the Mississippi river basin. *J. Hydrometeor.,* **1,** 88–94.

Seth, A., and F. Giorgi, 1998: The effects of domain choice on summer precipitation simulation and sensitivity in a regional climate model. *J. Climate,* **11,** 2698–2712.

Shepherd, J. M., B. S. Ferrier, and P. S. Ray, 2001: Rainfall morphology in Florida convergence zones: A numerical study. *Mon. Wea. Rev.,* **129,** 177–197.

Staniforth, A., 1997: Regional modeling: A theoretical discussion. *Meteor. Atmos. Phys.,* **63,** 15–29.

Takle, E. S., and Coauthors, 1999: Project to intercompare regional climate simulations (PIRCS): Description and initial results. *J. Geophys. Res.,* **104** (D16), 19 433–19 461.

Tripoli, G. J., and W. R. Cotton, 1982: The Colorado State University three-dimensional cloud/mesoscale model—1982. Part I: General theoretical framework and sensitivity experiments. *J. Rech. Atmos.,* **16,** 185–220.

Vinnikov, K. Y., A. Robock, N. A. Speranskaya, and C. A. Schlosser, 1996: Scales of temporal and spatial variability of midlatitude soil moisture. *J. Geophys. Res.,* **101,** 7163–7174.

von Storch, H., H. Langenberg, and F. Feser, 2000: A spectral nudging technique for dynamical downscaling purposes. *Mon. Wea. Rev.,* **128,** 3664–3673.

Waldron, K. M., J. Paegle, and J. D. Horel, 1996: Sensitivity of a spectrally filtered and nudged limited-area model to outer model options. *Mon. Wea. Rev.,* **124,** 529–547.

Walko, R. L., and Coauthors, 2000: Coupled atmosphere–biophysics–hydrology models for environmental modeling. *J. Appl. Meteor.,* **39,** 931–944.

Wang, M., J. Paegle, and S. DeSordi, 1999: Global variable resolution simulations of Mississippi river basin rains of summer 1993. *J. Geophys. Res.,* **104** (D16), 19 399–19 414.

Warner, T. T., R. A. Paterson, and R. E. Treadon, 1997: A tutorial on lateral boundary conditions as a basic and potentially serious limitation to regional numerical weather prediction. *Bull. Amer. Meteor. Soc.,* **78,** 2599–2617.